

# Optical and magnetic properties of the photo-induced state in the coordination network $\text{Na}_2\text{Co}_4[\text{Fe}(\text{CN})_6]_{3.3} \cdot 14\text{H}_2\text{O}^\dagger$

Rémy Le Bris,<sup>ab</sup> Jean-Daniel Cafun,<sup>c</sup> Corine Mathonière,<sup>\*ab</sup> Anne Bleuzen<sup>c</sup> and Jean-François Létard<sup>ab</sup>

Received (in Montpellier, France) 11th February 2009, Accepted 17th April 2009

First published as an Advance Article on the web 7th May 2009

DOI: 10.1039/b902833a

The study of the metastable state, obtained by light irradiation of  $\text{Na}_2\text{Co}_4[\text{Fe}(\text{CN})_6]_{3.3} \cdot 14\text{H}_2\text{O}$  is reported using reflectivity and magnetic measurements. This compound is characterized by a charge transfer phenomenon occurring between a high-temperature phase (HT phase) formed by paramagnetic  $\text{Co}^{\text{II}}\text{--Fe}^{\text{III}}$  pairs and a low-temperature phase (LT phase) formed by diamagnetic  $\text{Co}^{\text{III}}\text{--Fe}^{\text{II}}$  pairs with the occurrence of a thermal-induced hysteresis loop. A metastable phase can be also formed at low temperature by irradiation following a photo-induced charge transfer between the LT phase and the photo-induced phase (PI phase) formed by  $\text{Co}^{\text{II}}\text{--Fe}^{\text{III}}$  pairs. The phenomenon corresponds to the well-known light-induced excited spin state trapping (LIESST) effect. The study of the dynamics in the PI phase showed that the relaxation curves follow monoexponential decays. This is in apparent contradiction with the presence of a thermal hysteresis loop. The thermodynamic parameters that govern the relaxation have been determined. The accuracy of these parameters has been checked by simulating the experimental  $T(\text{LIESST})$  curve.

## Introduction

The photocontrol of magnetic states is a very active field of research in molecular compounds because it opens opportunities for using these compounds in magneto-optical devices.<sup>1</sup> Two electronic phenomena are known to generate photomagnetic properties in the solid state: the spin crossover (SCO) for a  $3d^n$  transition metal ion ( $n = 4\text{--}7$ )<sup>2</sup> and the electron transfer (ET) between two transition metal ions<sup>3</sup> or between one transition metal ion and one ligand.<sup>4</sup> Despite the fact that the two phenomena (SCO and ET) are very different at the atomic level, some analogies exist in the bulk materials.<sup>1,5,6</sup> Both can be thermally induced to give a conversion (or transition) between a *low-spin* state at low temperature and a *high-spin* state at high temperature. The driving force of the conversion is brought by the entropy associated to a higher electronic degeneracy in the high-spin state. Moreover, it has been demonstrated that it was possible for some compounds exhibiting SCO and ET phenomena to populate by light irradiation the high-temperature state from the stable low-temperature state.<sup>3,7</sup> This light-induced excited spin state trapping is the so-called LIESST effect,<sup>7</sup> and has been reported for numerous SCO compounds.<sup>2a,6,8</sup> Actually

these photo-induced high-spin states are metastable states, and relax to the thermodynamic states through a thermally activated regime. The use of these switchable compounds in devices is strongly dependent to these relaxation processes because they determine the lifetime of the photogenerated state. Optical and magnetic techniques have been extensively used to study the relaxation dynamics in numerous SCO compounds.<sup>2</sup> Concerning the ET phenomenon, only few relaxation studies have been performed. These studies concern (i) Prussian Blue Fe–Co analogs with different alkali metal ions,<sup>9</sup> (ii) a Co–W(CN)<sub>8</sub> network,<sup>10</sup> and (iii) a molecular analog of CoFe networks.<sup>11</sup> In order to obtain the thermodynamic parameters that govern the relaxation processes and thus the lifetime of the photogenerated states, a careful study of the dynamics in these ET compounds must be carried out in a more systematic way.

In the present work, we have been interested in the complete description of the relaxation process that occurs in the photo-induced metastable phase in the compound  $\text{Na}_2\text{Co}_4[\text{Fe}(\text{CN})_6]_{3.3} \cdot 14\text{H}_2\text{O}$ . This compound has been selected among the large family of photosensitive Prussian Blue analogs for two reasons: (i) it displays a quantitative thermo-induced electron transfer,<sup>12</sup> (ii) it shows a thermal and a light-induced ET. In this work, we will describe the stable and metastable photo-induced phases by optical and magnetic techniques. Then, we will investigate in detail the relaxation of the magnetic metastable light-induced phase by determining the  $T(\text{LIESST})$  temperature<sup>13</sup> and by recording the kinetics as a function of time. Finally, we will simulate the thermal dependence of the magnetic properties in the light-induced state at a warming rate of  $0.3 \text{ K min}^{-1}$ .

<sup>a</sup> CNRS, UPR 9048, Institut de Chimie de la Matière Condensée de Bordeaux (ICMCB), 87 avenue du Dr. Albert Schweitzer, F-33608, Pessac, France. E-mail: mathon@icmcb-bordeaux.cnrs.fr; Fax: (+33) 5 40 00 27 61; Tel: (+33) 5 40 00 26 82

<sup>b</sup> Université de Bordeaux, UPR 9048, F-33608, Pessac, France

<sup>c</sup> Institut de Chimie Moléculaire et des Matériaux d'Orsay, Université Paris XI, CNRS UMR8182, 91405, Orsay, France

<sup>†</sup> Electronic supplementary information (ESI) available: X-Ray powder pattern and additional magnetic data of the compound. See DOI: 10.1039/b902833a

## Results

### Synthesis and structure

The synthesis of the title compound consists of the mixing of two aqueous solutions containing  $\text{Co}^{2+}$  ions and the  $[\text{Fe}(\text{CN})_6]^{3-}$  complex, in the presence of an excess of  $\text{NaNO}_3$ . The structure is typical of a non-stoichiometric phase in the well known Prussian Blue analogs (Scheme 1).<sup>14</sup> As shown by the powder X-ray diffraction pattern (Fig. S1, ESI†), the compound crystallizes in a face-centered cubic cell in the space group  $Fm\bar{3}m$  with a cell parameter  $a = 10.30 \pm 0.02$  Å. The three-dimensional network is made of an alternation of  $\text{Fe}(\text{CN})_6$  and Co ions, and due to the stoichiometry of the compound, there are 17.5%  $\text{Fe}(\text{CN})_6$  vacancies, which are filled with water molecules. Therefore the mean environment of the Co is  $\text{CoN}_5\text{O}$ .

### Optical studies

Solid-state reflectivity measurements were collected between 280 and 10 K. This technique allows to follow the optical spectra (absorbance and reflectance) of the material continuously irradiated with a white light of  $90 \text{ mW cm}^{-2}$ . Fig. 1 shows the thermal dependence of the absorption spectra during cooling from 280 to 30 K. At room temperature, the absorption spectrum shows a broad band with a maximum at 550 nm. This band is the result of the overlap of d–d transitions and the metal–metal charge transfer (MMCT) in the  $\text{Co}^{\text{II}}\text{–Fe}^{\text{III}}(\text{CN})_6$  system.<sup>15,16</sup> The absorption, below 700 nm, increases gradually down to 230 K, where a new absorption band appears around 760 nm. This band is the signature of the MMCT in the  $\text{Co}^{\text{III}}\text{–NC–Fe}^{\text{II}}$  pair.<sup>15</sup> Between 230 and 110 K, the spectra do not change. However, during cooling further below 110 K, a reverse process is observed suggesting a light-induced

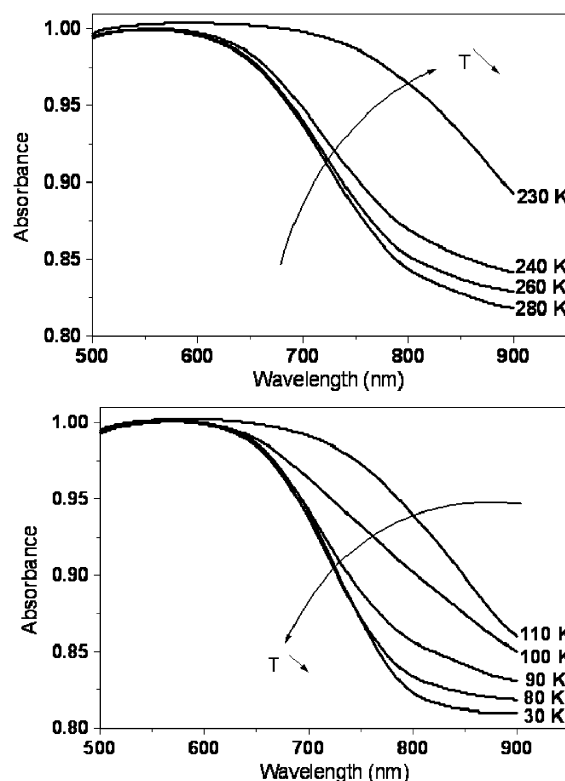
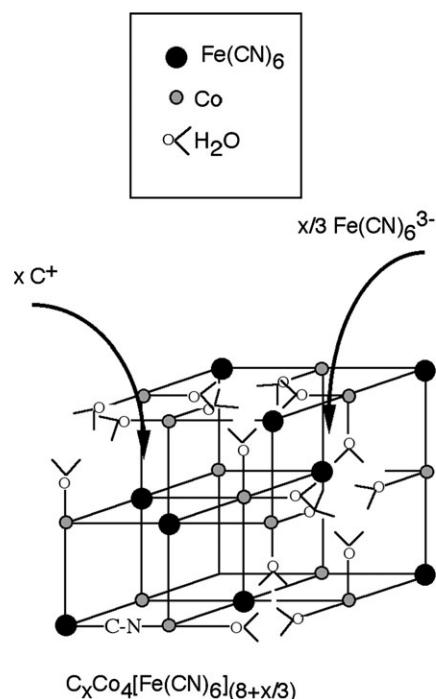


Fig. 1 Surface absorption spectra during cooling from 280 to 30 K.

phenomenon, with a gradual decrease of absorption below 700 nm. Finally, the spectra recorded at room temperature and at low temperature, 30 K, are similar. These optical changes are in agreement with a change of color of the material from reddish brown to purple when cooling from 300 to 100 K, and from purple to reddish brown at low temperature when it is irradiated.<sup>16</sup>

An alternative way to visualize these optical changes as a function of both temperature and light irradiation is presented in Fig. 2 in the form of the thermal dependence of the reflected light intensity by the sample in cooling and warming modes (with a sweeping rate of  $3 \text{ K min}^{-1}$ ) at a specific wavelength. The wavelength at  $800 (\pm 5) \text{ nm}$  has been selected because it is



Scheme 1 Structure of the Prussian Blue analog

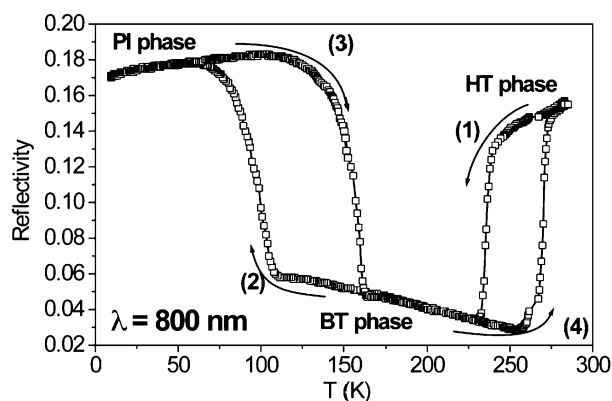


Fig. 2 Thermal dependence of the light intensity reflected by the sample at  $\lambda = 800 \pm 5 \text{ nm}$  during cooling ((1) and (2)) and warming ((3) and (4)) modes ( $3 \text{ K min}^{-1}$ ).

representative of the wavelengths in the 650–900 nm range. Upon cooling, the reflectivity shows first a decrease (arrow (1) on Fig. 2) from 0.16 at 280 K to 0.04 at 200 K. This value remains almost constant down to 120 K, but upon cooling further, the intensity starts to increase again (arrow (2)) to reach 0.17 at 10 K. Upon warming from 10 K, no change in the reflectivity appears up to 120 K. Beyond this temperature, the signal decreases (arrow (3)) to reach the previous observed value of 0.04 at 180 K. A last change appears above 250 K with an increase (arrow (4)) to recover the initial state at room temperature. The comparison between cooling and heating modes give rise to two thermal hysteresis loops: one at high temperature, and one at low temperature. This behaviour can be attributed for (1) and (4) to a thermal-induced transition between a high-temperature (HT) phase and a low-temperature (LT) phase, and, for (2) and (3) to a light-induced thermal hysteresis (= LITH),<sup>13</sup> between a LT phase and a photo-induced (PI) phase.

In summary, the photochromic and thermochromic properties of the sample are very similar to those obtained for other Prussian Blue analogs. As shown before,<sup>9a,b</sup> they are closely related to the magnetic changes. Therefore to go further in the interpretation of the optical data, a magnetic study has been carried out for the title compound.

### Magnetic studies

First, the magnetic studies have been performed in the dark by cooling the sample from 290 to 10 K, and then warming up (with a sweeping rate of 2 K min<sup>-1</sup>). The product of the molar magnetic susceptibility ( $\chi$ ) and the temperature vs. temperature is shown in Fig. 3.

At 290 K, the  $\chi T$  product is equal to 13.4 cm<sup>3</sup> K mol<sup>-1</sup>. This value corresponds to the expected value for 3.3 Fe(III) metal ions (d<sup>5</sup>, low spin,  $S = 1/2$ ,  $g = 2.7$ ) and 4 Co(II) metal ions in a high spin state (d<sup>7</sup>, high spin  $S = 3/2$ ,  $g = 2.55$ ). When the compound is cooled, a rapid decrease of  $\chi T$  is observed at  $T_{1/2}(\downarrow) \approx 243$  K. Below 220 K, the  $\chi T$  product is equal to 2.20 cm<sup>3</sup> K mol<sup>-1</sup> which is consistent with 3.3 diamagnetic

units Co<sup>III</sup>(3d<sup>6</sup>, low spin,  $S = 0$ )–NC–Fe<sup>II</sup>(3d<sup>6</sup>, low spin,  $S = 0$ ) and 0.7 Co(II) metal ion in a high spin state. In heating mode, a thermal hysteresis loop is observed with a rapid increase of  $\chi T$  at  $T_{1/2}(\uparrow) \approx 272$  K. This magnetic hysteresis loop is similar to the optical hysteresis above 200 K. Therefore, the optical loop observed above 200 K is only due to thermal effects on the properties. We can conclude that a thermal-induced phase transition between the HT phase (formulated as Na<sub>2</sub>Co<sup>II</sup><sub>4</sub>[Fe<sup>III</sup>(CN)<sub>6</sub>]<sub>3.3</sub>·14H<sub>2</sub>O) and the LT phase (formulated as Na<sub>2</sub>Co<sup>II</sup><sub>0.7</sub>Co<sup>III</sup><sub>3.3</sub>[Fe<sup>II</sup>(CN)<sub>6</sub>]<sub>3.3</sub>·14H<sub>2</sub>O) is observed with a thermal hysteresis loop around 258 K and a width of  $\pm 14.5$  K, due an electron transfer between Co and Fe.

Let us now consider the light-induced effect on magnetic properties. At low temperature (10 K), upon irradiation with a red laser beam ( $\lambda = 647$  nm) on a thin layer of the compound, the magnetic response was observed to immediately increase, and after 2 h, a photostationary point was reached (Fig. S2, ESI†). Fig. 3 presents the magnetic response under 0.5 T of the photo-induced phase (PI phase) when the light is switched off and the temperature is increased (with a warming rate of 0.3 K min<sup>-1</sup>). The  $\chi T$  plot of the PI phase presents three different steps. At low temperatures, the  $\chi T$  product first increases from 52 cm<sup>3</sup> K mol<sup>-1</sup> (10 K) to 65 cm<sup>3</sup> K mol<sup>-1</sup> (50 K), then decreases to become more or less constant in the range 50–110 K with a value around 15 cm<sup>3</sup> K mol<sup>-1</sup>. The existence of a maximum in the  $\chi T$  vs.  $T$  plot is due to the appearance of magnetic ordering in the PI state.<sup>17</sup> Actually, the light excitation induced an electron transfer from the low-spin Fe<sup>II</sup> ion to the low-spin Co<sup>III</sup> ion, giving rise to paramagnetic Fe<sup>III</sup> and Co<sup>II</sup> ions. The magnetic interactions between Fe<sup>III</sup> and Co<sup>II</sup> ions leads to a magnetic ordering in the PI phase with a Curie temperature at 21 K, as already reported for this material.<sup>18</sup> Finally, when the temperature is increased further, the  $\chi T$  product of the PI phase decreases rapidly to recover around 140 K the  $\chi T$  value of the LT phase (2.80 cm<sup>3</sup> K mol<sup>-1</sup>). This curve allows the determination for the PI phase of the  $T(\text{LIESST})$ ,<sup>6,13,19</sup> which is the minimum of the  $d(\chi T)/dT$  vs.  $T$  plot when the temperature increased at a rate of 0.3 K min<sup>-1</sup>. For the present compound,  $T_{1/2}$  is 258 K and  $T(\text{LIESST})$  is 128 K (Fig. 3).

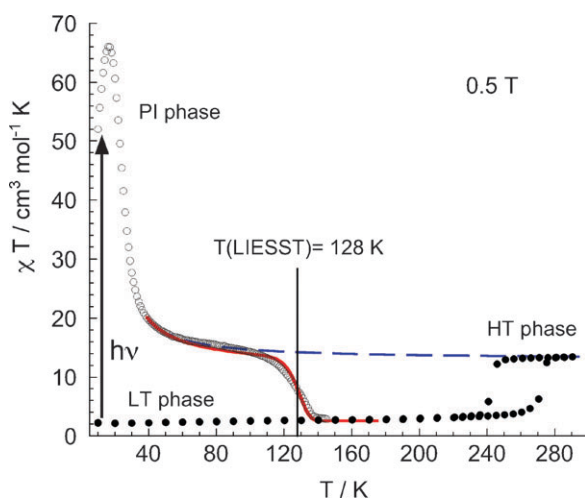


**Fig. 3** Thermal dependence of the  $\chi T$  product vs. temperature: (●) before light irradiation; (○) after irradiation at 10 K during 2 h with  $\lambda = 647$  nm; (---)  $(\chi T)_{\text{mag}}$ ; (—)  $T(\text{LIESST})$  simulation.

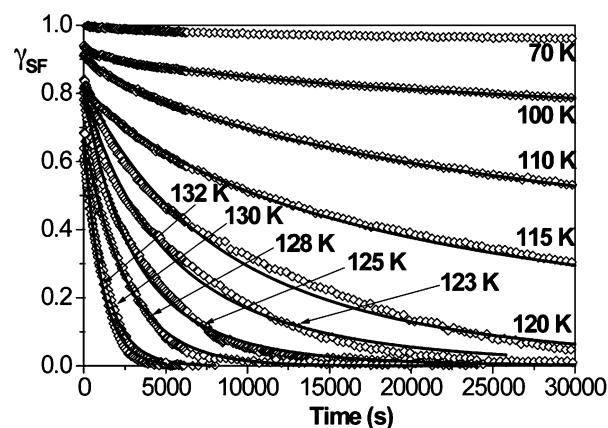


**Fig. 4** Relaxation kinetics of the PI phase recorded at different temperatures. Lines correspond to fits with a monoexponential decrease.

To obtain the thermodynamic parameters governing the dynamics in the PI state, we have carried out kinetics studies using the magnetic technique. The relaxation kinetics of the PI  $\rightarrow$  LT phase transformation occurring after the irradiation at 10 K have been performed in the range 70–132 K. Fig. 4 shows the time dependence of the switching fraction rate in the PI phase, denoted  $\gamma_{\text{SF}}$ , at different temperatures. To determine the  $\gamma_{\text{SF}}$  rate, we used the following method: (i) we assumed that the PI phase was quantitatively photo-generated at low temperatures, *i.e.* below 60 K; (ii) then, we determined an analytical expression of the  $\chi T$  product using the parameters obtained with the fit of  $1/\chi$  for a ferrimagnetic material above its Curie temperature (Fig. S3, ESI†).<sup>20</sup> The deduced expression  $(\chi T)_{\text{mag}}$  is supposed to be valid above 40 K, and would correspond to an hypothetical HT phase in the entire temperature range.<sup>21</sup> The thermal evolution of  $(\chi T)_{\text{mag}}$  is presented in Fig. 3. Finally, we determine for each temperature  $\gamma_{\text{SF}}$  as the  $[(\chi T) - (\chi T)_{\text{LT}}]/[(\chi T)_{\text{mag}} - (\chi T)_{\text{LT}}]$  ratio.

In Fig. 4, we observe two different thermal regions for the relaxation. Below 90 K, the relaxation is nearly temperature independent. For instance, for the PI state at 70 K, the relaxation process represents less than 2% after 10 h. This suggests that the relaxation process is governed by the quantum-tunnelling regime.<sup>22</sup> The rate constant  $k_{\text{HL}}(T \rightarrow 0)$ , which characterizes the relaxation in the quantum tunnelling regime, is estimated as an upper limit of  $k_{\text{HL}}$  determined from the last complete kinetic measurement recorded at low temperature, *i.e.* at 100 K ( $k_{\text{HL}}(T \rightarrow 0) = 0.1 \times 10^{-5} \text{ s}^{-1}$ , Table 1). Above 100 K, the kinetics curves clearly show a monoexponential decay (eqn (1)), which can be satisfactorily fitted using a single exponential law (solid lines in Fig. 4).

$$k_{\text{HL}}(T) = k_{\text{HL}}(T \rightarrow \infty) \exp(-E_a/kT) \quad (1)$$

In this temperature range, the process is governed by the thermally activated regime. This enables us to extract at each temperature, the relaxation rate  $k_{\text{HL}}$  and also the lifetime  $\tau = (k_{\text{HL}})^{-1}$  of the PI state, as reported in Table 1.

Parameters extracted from experimental data lead to a convenient Arrhenius plot of  $\ln(k_{\text{HL}}(T))$  vs.  $1/T$  (Fig. 5). A linear fit allows to determine the activation energy  $E_a = 2160 \text{ cm}^{-1}$  and frequency factor  $k_{\text{HL}}(T \rightarrow \infty) = 1.6 \times 10^7 \text{ s}^{-1}$  for the PI phase.

One way to test the coherence of the kinetic description is to use the kinetic parameters for reproducing the experimental  $\chi T$  vs.  $T$  curve in the light-induced state, named in our previous

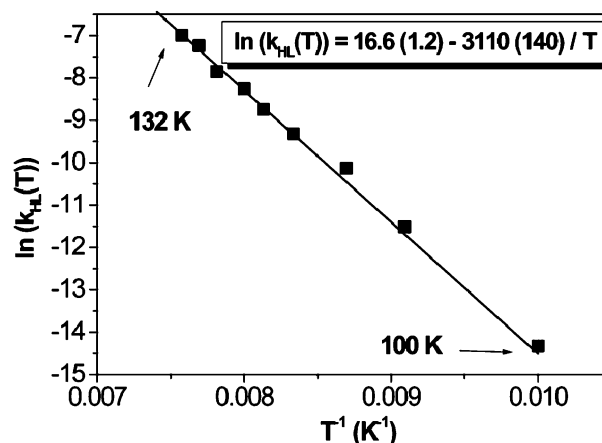


Fig. 5 Arrhenius plot obtained from the parameters extracted from the relaxation curves shown in Fig. 4.

work as the  $T(\text{LIESST})$  curve.<sup>6,19,23</sup> We have demonstrated that the time dependence of the switching fraction at temperature  $T_i$  can be obtained by eqn (2):<sup>6b,23</sup>

$$\left(\frac{\partial \gamma_{\text{SF}}}{\partial t}\right)_{T_i} = -\gamma_{\text{SF}} \{k_{\text{HL}}(T \rightarrow 0) + k_{\text{HL}}(T \rightarrow \infty) \exp(-E_a/k_B T_i)\} \quad (2)$$

Finally, we have to take into account the existence of magnetic interactions at low temperature. For that we have used the analytical expression simulated for a hypothetical HT phase in all the measured temperature range above  $\chi T_{\text{mag}}$ .<sup>20</sup> The  $T(\text{LIESST})$  curve is then expressed according to eqn (3)

$$\chi T = \chi T_{\text{mag}} \gamma_{\text{SF}} \quad (3)$$

Fig. 3 shows the calculated  $T(\text{LIESST})$  curve in the PI state. The rate constant of the tunnelling region,  $k_{\text{HL}}(T \rightarrow 0)$ , the pre-exponential factor,  $k_{\text{HL}}(T \rightarrow \infty)$ , the activation energy of the thermally activated region,  $E_a$ , used are those obtained from the experimental kinetics. The agreement with the experimental data is good. The shape and the capacity of the compound to retain the trapped-induced HT information, estimated through the determination of the  $T(\text{LIESST})$ , are well described.

## Discussion

In the present work we have reported the photomagnetic properties of  $\text{Na}_2\text{Co}_4[\text{Fe}(\text{CN})_6]_{3.3} \cdot 14\text{H}_2\text{O}$ . The first observation, that we can address, concerns the optical and magnetic signals recorded in the PI state between 50 and 100 K (*i.e.* where magnetic ordering can be neglected) which are close to the values measured in the HT phase. This confirms that the light-conversion is quantitative at the surface and in the bulk of the material.

The second observation concerns the occurrence of a hysteresis loop in the thermal-induced phase transition of  $\text{Na}_2\text{Co}_4[\text{Fe}(\text{CN})_6]_{3.3} \cdot 14\text{H}_2\text{O}$ , observed by optical and magnetic measurements. This is indicative of a certain degree of cooperativity, in agreement with the results of other sodium and rubidium Fe–Co Prussian Blue analogs.<sup>9,24</sup> Actually, it

Table 1 Relaxation rates extracted at each temperature from the fitting of the relaxation curves

$T/\text{K}$	$T^{-1}/\text{K}^{-1}$	$10^5 k_{\text{HL}}/\text{s}^{-1}$	$\tau/\text{s}$
100	0.01	0.10	1 000 000
110	0.00909	1.0	100 000
115	0.00869	4.0	25 000
120	0.00833	9.0	11 111
123	0.00813	16.0	6250
125	0.008	26.0	3846
128	0.00781	39.0	2564
130	0.00769	72.0	1389
132	0.00758	92.0	1087



has been established by X-ray spectroscopies<sup>25</sup> performed for some of these systems that the electron transfer between the  $\text{Fe}^{\text{III}}\text{--CN--Co}^{\text{II}}$  and  $\text{Fe}^{\text{II}}\text{--CN--Co}^{\text{III}}$  pairs is accompanied by an important decrease in Co–N bond lengths from 2.1 Å in the HT phase to 1.9 Å in the LT phase. This decrease at the atomic level has important effect on neighbours in the 3D network by the means of elastic interactions. If we now consider the PI phase, our results contrast with the previous works.<sup>9</sup> The relaxation curves already published showed a deviation from mono-exponential decays with sigmoidal shapes. They have been analyzed with a self-accelerated process due to cooperative effects on the relaxation rates. The self acceleration is explained by an internal pressure into the lattice accompanying the relaxation process and a progressive lowering of the energy barrier of the metastable states.<sup>26</sup> Our experimental results are different (Fig. 4): the relaxation curves in the PI state have been satisfactorily fitted with mono-exponential decays. This type of relaxation is shown usually for non-cooperative systems. However, the reflectivity measurements with a scan rate of 3 K min<sup>−1</sup> of  $\text{Na}_2\text{Co}_4[\text{Fe}(\text{CN})_6]_{3.3}\cdot 14\text{H}_2\text{O}$  reveal the existence at low temperature of a light-induced thermal hysteresis loop (Fig. 2). In previous works, the origin of LITH loops has been attributed to the competition between the constant photo-excitation and the thermal relaxation process in a cooperative material.<sup>9c,27</sup> Therefore, at this stage of our study, we can not decide unambiguously about the cooperative character of the PI phase. The study of the relaxation decays suggests the absence of significant cooperativity despite the measurement of a LITH loop under constant irradiation.

To go further, we performed a new experiment to minimize the kinetic effects. Actually, to check if the LITH loop measured by reflectivity is not simply due to a too rapid scan rate, we have recorded the magnetic properties by cooling and warming the sample under constant irradiation at a lower scan rate of 0.1 K min<sup>−1</sup>. The results are shown in Fig. 6, and confirm the existence of an apparent LITH loop. To approach the real LITH loop,<sup>23</sup> *i.e.* the steady state between the population and the relaxation processes, we have

determined the photostationary points on both cooling and warming branches at 110 K (inset of Fig. 6). For the cooling branch, the sample was slowly cooled down to 110 K. The sample was then irradiated, and the time dependence of  $\chi T$  plot was recorded. The experiment was stopped when a photostationary limit was reached with a  $\chi T$  value of 7.5 cm<sup>3</sup> mol<sup>−1</sup> K. For the heating branch, the sample was irradiated at 10 K until saturation, then warmed at 110 K, and at 110 K, the time dependence of  $\chi T$  plot was recorded. A new photostationary limit is reached with a  $\chi T$  value of 12 cm<sup>3</sup> mol<sup>−1</sup> K. Based on these experiments, it is now clear that  $\text{Na}_2\text{Co}_4[\text{Fe}(\text{CN})_6]_{3.3}\cdot 14\text{H}_2\text{O}$  displays a real LITH loop, suggesting a cooperative behaviour. Now, it remains to explain why the relaxation curves do not present a cooperative character as expected. This apparent inconsistency has already been observed in a SCO  $\text{Fe}^{2+}$  compound.<sup>28</sup> This compound presents a steep spin transition with a narrow thermal hysteresis loop, a LITH loop and a stretched exponential nature of the relaxation curves ascribed usually to some structural disorder. In this last example, the authors have proposed that the disorder caused by the structural phase transition at low temperature, hides the cooperative character of the relaxation curves. In our case, the situation is certainly also complex. The disorder may be assigned to the non-stoichiometric character of the compound.<sup>9d,e</sup> The present idea is that in  $\text{Na}_2\text{Co}_4[\text{Fe}(\text{CN})_6]_{3.3}\cdot 14\text{H}_2\text{O}$  the existence of small composition defects is important enough to reduce the effects of interactions in the lattice and consequently hide the cooperative character of the PI phase. Further work is currently in progress to understand this unusual behaviour.

Concerning now the challenge of addressing optical perturbation on a molecular magnetic material at room temperature outside the thermal hysteresis loop,<sup>2e</sup> the system reported in this work possesses a long lifetime in the metastable phase. All the other compounds showing longer lifetimes belong to the same family of Prussian Blue, namely  $\text{Na}_x\text{Co}_4[\text{Fe}(\text{CN})_6]_y$ . For example, the lifetime has been spectroscopically determined at 170 K, for the compound  $\text{Na}_{1.85}\text{Co}_4[\text{Fe}(\text{CN})_6]_{3.4}\cdot 4\text{H}_2\text{O}$ , as  $\tau = 10$  ms. Using the thermodynamic parameters determined in this study, we can calculate for  $\text{Na}_2\text{Co}_4[\text{Fe}(\text{CN})_6]_{3.3}\cdot 14\text{H}_2\text{O}$ , a lifetime  $\tau(170\text{ K}) = 4.7$  s. Only, one octanuclear compound  $\{[(\text{pzTp})\text{FeCN}_3]_4\}[\text{Co}(\text{pz})_3\text{CCH}_2\text{OH}]_4[\text{ClO}_4]_4$ , which corresponds to the molecular analogue of the FeCo network has a longer lifetime in the light-induced state reported so far, with  $\tau(170\text{ K}) = 6253$  s.<sup>11</sup> These results show the important role that the Fe–CN–Co system can play for the generation of compounds with long lifetimes in the photo-induced states.

Finally, the analogy of the properties of the studied compound with the spin-crossover compounds allows us to add this compound in the existing database  $T(\text{LIESST}) = f(T_{1/2})$  for the spin crossover compounds.<sup>6,19</sup> The data for the present compound is in good agreement with the results given by Hashimoto *et al.* on similar Na Prussian Blue analogues.<sup>29</sup> The long lifetime in the metastable state of the present compound gives rise to one of the highest  $T(\text{LIESST})$  reported so far. In a future work, we will include other photomagnetic Prussian Blue analogues in the  $T(\text{LIESST})$  data base which can be easily extended to charge transfer compounds.

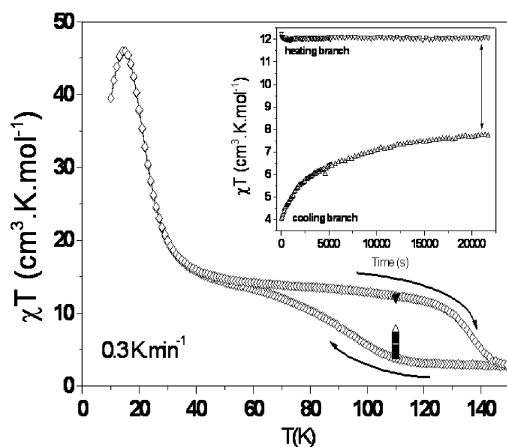


**Fig. 6** Thermal dependence of the  $\chi T$  product vs. temperature under constant irradiation. Inset: time dependence of the  $\chi T$  product vs. time on cooling and heating branches.

## Conclusions

In this study, we report the detailed study of the metastable phase generated by light irradiation in  $\text{Na}_2\text{Co}_4[\text{Fe}(\text{CN})_6]_{3.3} \cdot 14\text{H}_2\text{O}$ . We have shown that the charge transfer can be quantitatively induced by temperature and red-light irradiation in this FeCo Prussian Blue analog. We have been able to determine the thermodynamic parameters governing the relaxation process. Presently, new systems based on Fe–CN–Co are under investigation to understand the physical and chemical factors that govern the thermal long lifetimes of the photo-induced states.

## Experimental

### Synthesis of the complex $\text{Na}_2\text{Co}_4[\text{Fe}(\text{CN})_6]_{3.3} \cdot 14\text{H}_2\text{O}$

The compound was prepared according to the literature.<sup>29</sup> An aqueous solution (200 mL) of a  $\text{Co}^{\text{II}}$  salt (0.01 M) was added to a mixed aqueous solution (50 mL) of  $[\text{Fe}^{\text{III}}(\text{CN})_6]$  (0.015 M) and a solution of  $\text{NaNO}_3$  (0.06 M) at room temperature. The brown precipitated powder was filtered off, washed with water and allowed to dry in air. The elemental analysis confirmed that the formula was  $\text{Na}_2\text{Co}_3[\text{Fe}(\text{CN})_6]_{3.3} \cdot 14\text{H}_2\text{O}$ : Calc.: Na, 3.73; Co, 19.11; Fe, 14.94; C, 19.28; H, 2.29; N, 22.49%. Found: Na, 3.48; Co, 17.51; Fe, 14.07; C, 17.85; H, 2.07; N, 23.41%.

### Optical studies

The optical properties were investigated using a home-built reflectivity system equipped with a CVI spectrometer which allows us first, to collect reflectivity spectra, within the range of 500–900 nm, at different temperatures, then, second, to observe the temperature dependence of the signal at fixed wavelengths ( $\pm 2.5$  nm) between 10 and 290 K. The scanning rate in temperature is  $3 \text{ K min}^{-1}$ . Experiments were performed on a thin layer of powder.

### Magnetic measurements

The magnetic properties were carried out with a MPMS-5S Quantum Design SQUID (Superconducting Quantum Interference Device) magnetometer operating with an external magnetic field of 0.5 T within the range of 10–290 K. The measurements were performed on a sample of 9.7 mg placed in a gelatine cap. The experimental data were corrected for the diamagnetic contribution by using Pascal's constants.<sup>30</sup>

Photomagnetic measurements were performed using a Spectrum Physics Beam lock 2060 laser ( $\lambda = 647 \text{ nm}$ ) coupled via an optical fibre to the cavity of a MPMS-5S Quantum Design SQUID magnetometer. Photomagnetic samples consisted of a thin layer of compound whose weight was obtained by comparison of the curve obtained with a more accurately weighed sample of the same material (see above).<sup>6b</sup> The sample was irradiated ( $\lambda = 647 \text{ nm}$ ) at  $T = 10 \text{ K}$  during 2 h. The optical power at the sample surface was adjusted to  $5 \text{ mW cm}^{-2}$ , in order to minimize the heating of the sample. For the relaxation studies, the compound is irradiated at 10 K during 2 h, and then warmed to the desired temperature to follow the kinetics with the light switch on. When the desired

temperature is stable, the light is switched off, and the kinetics is started.

The  $T(\text{LIESST})$  curve is determined by following the previously published standardised methods described for iron(II) spin-crossover materials.<sup>6,19,23</sup> It consists of warming the sample at a rate of  $0.3 \text{ K min}^{-1}$  and recording the magnetisation at each 1 K interval.

## Acknowledgements

This work was supported by the CNRS, the University of Bordeaux, MAGMANet (NMP3-CT-2005-515767), the GDR MCM (Magnetisme et Commutation Moléculaires) and the Conseil Régional d'Aquitaine for supporting at the ICMCB the development of the ICPA platform (International Center of Photomagnetism in Aquitaine).

## References

- (a) O. Sato, J. Tao and Y.-Z. Zhang, *Angew. Chem., Int. Ed.*, 2007, **46**, 2152; (b) A. Dei, *Angew. Chem., Int. Ed.*, 2005, **44**, 1160.
- (a) See for general reviews: *Spin Crossover in Transition Metal Compounds, Topics in Current Chemistry*, ed. P. Gülich and H. A. Goodwin, Springer Verlag, Berlin-Heidelberg-New York, 2004, vols. 233–235; (b) P. Gülich, A. Hauser and H. Spiering, *Angew. Chem., Int. Ed. Engl.*, 1994, **33**, 2024; (c) O. Kahn and C. J. Martinez, *Science*, 1998, **279**, 44; (d) P. Gülich, Y. Garcia and T. Woike, *Coord. Chem. Rev.*, 2001, **219–221**, 839; (e) J.-F. Létard, P. Guionneau and L. Goux-Capes, *Top. Curr. Chem.*, 2004, **235**, 221.
- O. Sato, T. Iyoda, A. Fujishima and K. Hashimoto, *Science*, 1996, **272**, 704.
- D. M. Adams, A. Dei, A. L. Rheingold and D. N. Hendrickson, *J. Am. Chem. Soc.*, 1993, **115**, 8221.
- F. Varret, K. Boukheddaden, E. Codjovi and A. Goujon, *Hyperfine Interact.*, 2005, **165**, 37.
- (a) J.-F. Létard, P. Guionneau, O. Nguyen, J. S. Costa, S. Marcen, G. Chastanet, M. Marchivie and L. Capes, *Chem.–Eur. J.*, 2005, **11**, 4582; (b) J.-F. Létard, *J. Mater. Chem.*, 2006, **16**, 2550.
- (a) S. Decurtins, P. Gülich, C. P. Köhler, H. Spiering and A. Hauser, *Chem. Phys. Lett.*, 1984, **105**, 1; (b) A. Hauser, *Chem. Phys. Lett.*, 1984, **124**, 543.
- (a) A. Hauser, *Coord. Chem. Rev.*, 1991, **111**, 275; (b) F. Varret, M. Nogues and A. Goujon, *Magnetism: Molecules to Materials*, ed. M. Drillon and J. S. Miller, Wiley–VCH, Weinheim, 2001, vol. 1, p. 257.
- (a) A. Goujon, O. Roubeau, F. Varret, A. Dolbecq, A. Bleuzen and M. Verdager, *Eur. Phys. J. B*, 2000, **14**, 115; (b) A. Goujon, F. Varret, V. Escax, A. Bleuzen and M. Verdager, *Polyhedron*, 2001, **20**, 1339; (c) F. Varret, K. Boukheddaden, E. Codjovi, I. Maurin, H. Tokoro, S. Ohkoshi and K. Hashimoto, *Polyhedron*, 2005, **24**, 2857; (d) S. Gawali-Salunke, F. Varret, I. Maurin, C. Enaschescu, M. Malarova, K. Boukheddaden, E. Codjovi, H. Tokoro, S.-I. Ohkoshi and K. Hashimoto, *J. Phys. Chem. B*, 2005, **109**, 8251; (e) M. Castro, J. A. Rodriguez-Velamazán, K. Boukheddaden, F. Varret, H. Tokoro and S.-I. Ohkoshi, *Europhys. Lett.*, 2007, **79**, 27007.
- R. Le Bris, C. Mathonière and J.-F. Létard, *Chem. Phys. Lett.*, 2006, **426**, 380.
- D. Li, R. Clérac, O. Roubeau, E. Harte, C. Mathonière, R. Le Bris and S. M. Holmes, *J. Am. Chem. Soc.*, 2008, **130**, 2152.
- A. Bleuzen, V. Escax, J.-P. Itié, P. Münsch and M. Verdager, *C. R. Chim.*, 2003, **6**, 343–352.
- J.-F. Létard, P. Guionneau, L. Rabardel, J. A. K. Howard, A. E. Goeta, D. Chasseau and O. Kahn, *Inorg. Chem.*, 1998, **37**, 4432.
- (a) A. Ludi and H. U. Güdel, *Struct. Bonding (Berlin, Ger.)*, 1973, **137**, 577; (b) M. Verdager, G. S. Girolami, *Magnetism: Molecules to Materials*, ed. J. S. Miller and M. Drillon, Wiley–VCH, 2005, vol. V, p. 283.

- 15 C. Berlinguette, A. Dragulescu-Andrasi, A. Z. Siebezr, H.-U. Güdel and C. Achim. K. Dunbar, *J. Am. Chem. Soc.*, 2005, **127**, 6766.
- 16 Y. Sato, S.-I. Ohkoshi and K. Hashimoto, *J. Appl. Phys.*, 2002, **92**, 4834.
- 17 O. Sato, Y. Einaga, A. Fujishita and K. Hashimoto, *Inorg. Chem.*, 1999, **38**, 4405.
- 18 J.-D. Cafun, G. Champion, M.-A. Arrio, C. Cartier dit Moulin and A. Bleuzen, manuscript in preparation.
- 19 (a) J.-F. Létard, L. Capes, G. Chastanet, N. Moliner, S. Létard, J. A. Real and O. Kahn, *Chem. Phys. Lett.*, 1999, **313**, 115; (b) S. Marcen, L. Lecren, L. Capes, H. A. Goodwin and J.-F. Létard, *Chem. Phys. Lett.*, 2002, **358**, 87.
- 20 L. Néel, *Ann. Phys.*, 1948, **t. 3**, 10.
- 21  $(\chi_M T)_{\text{mag}} = 14(T + 5)T/((T + 5)(T - 5) - (30 \times 14))$ ,  $C = 14 \text{ cm}^3 \text{ mol}^{-1} \text{ K}$  (Curie constant =  $3.3C(\text{Fe}^{3+}) + 4C(\text{Co}^{2+})$ ),  $\theta = -5 \text{ K}$ ,  $\gamma = 30 \text{ K}$ .
- 22 E. Bucks, M. Bixon and J. Jortner, *J. Am. Chem. Soc.*, 1980, **102**, 2918.
- 23 J.-F. Létard, G. Chastanet, O. Nguyen, S. Marcen, M. Marchivie and P. Guionneau, *Monatsh. Chem.*, 2003, **134**, 165.
- 24 T. Yamauchi, A. Nakamura, Y. Moritomo, T. Hozumi, K. Hashimoto and S. Ohkoshi, *Phys. Rev. B*, 2005, **72**, 214425.
- 25 (a) C. Cartier dit Moulin, F. Villain, A. Bleuzen, M.-A. Arrio, P. Saintavit, C. Lomenech, V. Escax, F. Baudalet, E. Dartyge, J.-J. Gallet and M. Verdaguer, *J. Am. Chem. Soc.*, 2000, **122**, 6653; (b) T. Yokohama, M. Kiguchi, T. Ohta, O. Sato, Y. Einaga and K. Hashimoto, *Phys. Rev. B*, 1999, **60**, 9340; (c) T. Yokohama, T. Ohta, O. Sato and K. Hashimoto, *Phys. Rev. B*, 1998, **58**, 8257.
- 26 (a) T. Buchen, P. Gülich and H. A. Goodwin, *Inorg. Chem.*, 1994, **33**, 4573; (b) A. Hauser, *Chem. Phys. Lett.*, 1992, **192**, 65.
- 27 (a) A. Desaix, O. Roubeau, J. Jeftic, J. G. Haasnoot, K. Boukheddaden, E. Codjovi, J. Linares, M. Nogues and F. Varret, *Eur. Phys. J. B*, 1998, **6**, 183; (b) C. Enachescu, H. Constant-Machado, E. Codjovi, J. Linares, K. Boukheddaden and F. Varret, *J. Phys. Chem. Solids*, 2001, **62**, 1409.
- 28 V. Mishra, R. Mukherjee, J. Linares, C. Balde, C. Desplanches, J.-F. Létard, E. Collet, L. Toupet, M. Castro and F. Varret, *Inorg. Chem.*, 2008, **47**, 7577.
- 29 N. Shimamoto, S.-I. Ohkoshi, O. Sato and K. Hashimoto, *Inorg. Chem.*, 2002, **41**, 678.
- 30 O. Kahn, *Molecular Magnetism*, Wiley-VCH, New York, 1993.